

POLARIZATION AS A PROBE OF THICK DUST DISK IN EDGE-ON GALAXIES: APPLICATION TO NGC 891

KWANG-IL SEON^{1,2}

Draft version October 8, 2018

Abstract

Radiative transfer models were developed to understand the optical polarizations in edge-on galaxies, which are observed to occur even outside the geometrically thin dust disk, with a scale height of ≈ 0.2 kpc. In order to reproduce the vertically extended polarization structure, we find it is essential to include a geometrically thick dust layer in the radiative transfer model, in addition to the commonly-known thin dust layer. The models include polarizations due to both dust scattering and dichroic extinction which is responsible for the observed interstellar polarization in the Milky Way. We also find that the polarization level is enhanced if the clumpiness of the interstellar medium, and the dichroic extinction by vertical magnetic fields in the outer regions of the dust lane are included in the radiative transfer model. The predicted degree of polarization outside the dust lane was found to be consistent with that (ranging from 1% to 4%) observed in NGC 891.

Subject headings: galaxies: ISM – galaxies: magnetic fields – polarization – radiative transfer – scattering – dust, extinction

1. INTRODUCTION

It is well known that materials in late-type spiral galaxies are mostly concentrated at the galactic midplane. However, there have been many attempts to probe extraplanar dust existing outside the galactic midplane. High-resolution optical images have revealed filamentary dust complexes above the galactic midplane up to ~ 2 kpc in nearby edge-on spiral galaxies (Howk & Savage 1997, 1999, 2000; Alton et al. 2000; Rossa et al. 2004; Thompson et al. 2004). The filamentary structures are traced by absorption against the background starlight, thereby implying preferentially “dense” dust clouds with an optical depth of $\gtrsim 1$. Therefore, a relatively “diffuse” dust component, if any, was not detectable in these studies. The “diffuse” dust should appear as a faint extended reflection nebula illuminated by starlight when the scale height of the stars is smaller than that of the extraplanar dust. The ultraviolet (UV) reflection halo due to the extraplanar dust residing above the galactic plane was first discovered in NGC 891 (Seon & Witt 2012; Seon et al. 2014). Hodges-Kluck & Bregman (2014) and Hodges-Kluck et al. (2016) reported detection of the UV halos around many highly-inclined galaxies. Seon et al. (2014) and Shinn & Seon (2015) developed radiative transfer models for the UV maps of edge-on galaxies to estimate the spatial distribution and amount of the extraplanar dust.

Polarization maps in the visible and near-infrared (NIR) wavelengths also allow large-scale galactic dust distributions to be traced (Scarrott et al. 1990; Scarrott & Draper 1996; Fendt et al. 1996; Jones 1997; Montgomery & Clemens 2014). The polarization in the optical wavelengths arises from dust scattering of starlight and by dichroic extinction. Dichroic extinction is the selective attenuation of starlight as it passes through a media in which aspherical dust grains are aligned. Radiative torque and other processes tend to align the long axes of aspherical dust grains in a direction perpendicular to a magnetic field (e.g., Roberge 1996; Lazarian & Hoang

2007). The extinction cross section is larger along the longer axes of grains so that light is preferentially absorbed along that direction. This yields a net polarization parallel to the magnetic field direction. On the other hand, the scattered light is polarized perpendicular to the scattering plane, which gives a circular polarization pattern around the central source. In any case, the presence of dust grains is a necessary condition for polarization in the optical wavelengths.

In edge-on galaxies, for instance NGC 891 and NGC 4565, extended optical polarization features were found in the bulge/halo regions above the galactic midplane (Scarrott et al. 1990; Scarrott & Draper 1996; Fendt et al. 1996). If only a thin dust layer exists in the galactic plane, polarization arising from scattering and/or dichroic extinction is not expected to be detected at high altitudes. It is, therefore, interesting to investigate whether the extended optical polarization is caused by the extraplanar dust layer which is responsible for the UV reflection halo.

In this paper, Monte Carlo radiative transfer calculations are presented to investigate the polarization pattern observed in an edge-on galaxy, NGC 891. Large-scale geometry of the magnetic field in NGC 891 is also discussed to explain the observed polarization patterns.

2. RADIATIVE TRANSFER MODEL

In order to explain the extended polarization pattern observed above the dust lanes of edge-on galaxies, in particular, NGC 891, radiative transfer models of dust-scattered and direct starlight were calculated using the three-dimensional Monte Carlo radiative transfer code MoCafe (Seon et al. 2014; Seon 2015; Seon & Draine 2016). The code models multiple scatterings of photons and uses a scheme that includes “forced first scattering” to improve the calculation efficiency in optically thin medium, and a “peeling-off” technique to produce an image toward the observer. The basic Monte-Carlo algorithms have been described in detail by many authors (Bianchi et al. 1996; Gordon et al. 2001; Baes et al. 2011; Steinacker et al. 2013). The code was updated to take the polarization effect by dust scattering into account, using an algorithm similar to that described in Bianchi et al. (1996) and Peest et al. (2017). Benchmark tests

¹ Korea Astronomy and Space Science Institute, Daejeon, 34055, Korea; kiseon@kasi.re.kr

² Astronomy and Space Science Major, Korea University of Science and Technology, Daejeon, 34113, Korea

were performed as described in Peest et al. (2017) and results similar to theirs were obtained. The code was also verified using the polarization models given in Bianchi et al. (1996).

The dust grains are assumed to be spherical and to have a size distribution as given by the MRN model (Mathis et al. 1977): $n(a) \propto a^{-3.5}$ ($0.005\mu\text{m} < a < 0.25\mu\text{m}$), where a is the grain radius. The dielectric constants for the two dust compositions (astronomical silicates and graphites) are adopted from the ones given by Draine & Lee (1984) and updated by Draine (2003). All the relevant properties (absorption and scattering cross sections, albedo, and Mueller matrix) were calculated using the Mie scattering theory. We used the numerical phase functions that were calculated with the Mie theory, instead of using the approximate Henyey-Greenstein function. Polycyclic aromatic hydrocarbons are not included because they are not relevant for the present purpose.

The dichroic extinction is calculated according to a prescription given by Wood (1997) and Wood & Jones (1997). Jones (1989a) found that the magnitude of dichroic polarization at the K band (P_K) is roughly proportional to $2.23\tau_K^{3/4}$ (%) over a wide range of optical depths τ_K . Whittet et al. (2008) also found a similar relation between the polarization and optical depth: $P_K/\tau_K \approx 5.08\tau_V^{-0.52}$ (%). Wood (1997) and Wood & Jones (1997) assumed that the proportionality relation of Jones (1989a) holds over other wavelengths and obtained the polarization degree of $P_V = 1.3\tau_V^{3/4}$ (%) at the V band as a function of optical depth by combining the Serkowski law and the Milky Way interstellar extinction curve, as given in Jones (1989b). We also assume that the polarization relation measured at K holds at V, but adopted the relation found by Whittet et al. (2008), and derived the polarization degree of $P_V = 2.7\tau_V^{0.48}$ (%) as a function of optical depth. At each interaction point, the photon packet is polarized by an amount of $P_V \sin^2 \theta$ in a direction parallel to the local magnetic field. Here, θ is the angle between the photon propagation direction and the magnetic field direction at the interaction location. The photon packet is also polarized by an amount calculated through the Mueller matrix as it is scattered. The difference caused by the adopted dust models does not significantly alter the present results and will be discussed later.

The galaxy model is composed of two stellar (disk + bulge) and two dust (thin and thick disks) components. The stellar and dust disks are described by “double-exponential” distributions

$$\rho^{\text{disk}}(r, z) = \rho_0^{\text{disk}} \exp(-r/R - |z|/Z), \quad (1)$$

where ρ is the star or dust density at the radial and vertical coordinates r and z in the cylindrical coordinate system. ρ_0 is the density at the galactic center. The radial scale length and vertical scale height are denoted by R and Z , respectively. The luminosity density for the spheroidal bulge is given by the de-projection function of a Sersic profile. The density profile with a profile index n is given by

$$\rho^{\text{bulge}}(r, z) = \rho_0^{\text{bulge}} \exp(-b_n B^{1/n}) B^{-(2n-1)/2n}, \quad (2)$$

where

$$B = \frac{\sqrt{r^2 + z^2/q^2}}{R_e}. \quad (3)$$

Here, q is the minor to major axis ratio and R_e the effective radius. In this study, a de Vaucouleurs’ profile corresponding to a Sersic profile with $n = 4$ ($b_n = 7.67$) was used.

For the stellar and dust distributions, three types of models were investigated, as shown in Table 1. In the table, the optical depths of the dust disks are the central face-on optical depths of the exponential disks. Model A includes only a thin dust disk while Models B, C and D include an additional, geometrically thick dust disk. The model parameters for Model A are adopted from the best-fit values estimated for the V-band data of NGC 891 in Xilouris et al. (1999). The parameters for the thick dust disk, used to represent the extraplanar dust in Models B, C and D, were adopted from the best-fit model for the Far-UV observation as given by Seon et al. (2014). Model B is the same as Model A except that the bulge effective radius and the bulge-to-total luminosity ratio are slightly reduced compared to those of Model A. The bulge light scattered by the extraplanar dust disk makes the bulge appear bigger than it really is. Therefore, the bulge parameters of Model B were slightly reduced in order to produce a similar extent of the model galaxy as that obtained in Model B, as will be shown later.

We also calculated radiative transfer models (Models C and D) in a clumpy two-phase medium which consists of high-density clumps and a low-density inter-clump medium. In Models C and D, a “smooth” distribution of dust density $\langle \rho \rangle$ which is the same as that of Model B, was first produced. The probability of any cell being in a high-density state or a low-density state is randomly determined, based on the filling factor of the clumps ($f = 0.2$ and 0.15 for Models C and D, respectively). The high-density clumps are multiplied by a factor of $\rho_{\text{high}}/\langle \rho \rangle = 4$ (Model C) and 6 (Model D), and the low-density medium by a factor of $\rho_{\text{low}}/\langle \rho \rangle = (1 - f\rho_{\text{high}}/\langle \rho \rangle)/(1 - f) = 0.25$ (Model C) and 0.12 (Model D). The resulting medium is statistically the same as that of Model B. The medium for Model D is clumpier than that for Model C.

In general, edge-on galaxies show optical polarization within the dust lane with orientations parallel to the galactic plane (Scarrott et al. 1990; Scarrott 1996; Fendt et al. 1996; Jones 1997; Montgomery & Clemens 2014). On the other hand, polarization in the outer regions appears to be perpendicular to the galactic plane. These observational results imply that there is a large-scale toroidal magnetic field in the inner regions of galaxies and a vertical magnetic field in the outer regions. We, therefore, considered three cases with respect to the magnetic field geometry for each model type in Table 1. In the first case, no dichroic effect was included, to investigate the polarization effect due to pure scattering. In the second case, the magnetic field geometry was assumed to be toroidal, i.e., parallel to the galactic plane and perpendicular to the radial direction in the cylindrical coordinates. In the third case, the magnetic field was perpendicular to the galactic plane, to mimic a poloidal magnetic field geometry. The two magnetic field geometries are rather simple, but appear to be good enough to demonstrate the dependence of polarization pattern on the magnetic field geometry.

3. RESULTS

Figure 1 shows the simulated polarization maps at V for Model A, in which only a thin dust disk is included in the radiative transfer calculation. In the top panel, no dichroic extinction is included in the calculation. The polarization is found to be mostly vertical to the galactic plane (centrosymmetric around the bulge) and restricted within about $\pm 20''$ (± 1.0 kpc at the distance of NGC 891, 9.5 Mpc) from the plane. Degree of polarization is less than $\sim 1\%$. The highest

polarizations of $\sim 1\%$ occur within the dust lane ($|Y| \lesssim 5''$ or 0.25 kpc) from the plane. We also note that the polarization is weaker in the bulge region than in the outer regions. These are consistent with the previous results obtained for edge-on galaxy models in Bianchi et al. (1996) and Peest et al. (2017).

If the magnetic field is parallel to the galactic plane (middle panel), the polarization in the inner regions is very small and parallel to the galactic plane. This is attributed to dichroic extinction by dust grains aligned by toroidal magnetic fields. On the other hand, vertical polarizations are shown in the outer regions in which scattering is dominant. There are polarization null points near a radius of $100''$ in the dust lane. In the null points, the vertical polarization due to scattering is cancelled out by the parallel polarization due to the dichroic extinction along the toroidal magnetic field. The null points are indeed found in optical polarization maps of edge-on galaxies (Scarrott et al. 1990; Draper et al. 1995; Montgomery & Clemens 2014).

If the magnetic field is vertical to the plane (bottom panel), the dichroic polarization enhances the polarization degree due to scattering. However, in all three cases in Figure 1, the polarization is very small or negligible outside the dust lane. This is because the stellar scale height is much larger than the dust scale height. At high galactic altitudes, stars are viewed through a very small amount of dust and hence the polarization arising from scattering or dichroic extinction is very low.

The above models are, however, in contrast to the NIR and visible polarization maps, which show significant polarization structures outside the dust lane (Scarrott & Draper 1996; Scarrott 1996; Fendt et al. 1996; Jones 1997). In particular, a degree of polarization of up to 4% was found in the bulge/halo regions of NGC 891 by Fendt et al. (1996). The polarization patterns observed in the bulge/halo regions suggest the existence of a large scale dust layer above the midplane.

Figure 2 shows the results for the case in which an additional, thick dust disk with a scale height of 1.6 kpc and a central face-on optical depth of 0.3 at V is also included. It can be immediately recognized that the polarization signature is now visible even at the bulge and high altitudes in all three cases. In the middle panel, the null polarization points occur at about $100''$ in the dust lane, as in the middle panel of Figure 1. The degree of polarization is about 1.2–1.5 times higher than the case in which no thick dust disk is included. In the case of vertical magnetic field (bottom panel), up to $\sim 3\%$ polarization degree is found, which is close to the maximum polarization of $\sim 4\%$ measured in NGC 891 (Fendt et al. 1996). The polarization vectors within $\sim 50''$ from the galactic center are mainly perpendicular to the plane. It is also clear that the bottom panel with the vertical magnetic field shows higher degree of polarizations compared to the two other cases, in which the magnetic field is absent or parallel to the galactic plane. We also note that the degree of polarization in general rises with distance from the midplane, as observed in the optical polarization maps.

The galaxy models in Figures 1 and 2 consist of smooth dust and stellar components. For better models, we need to consider the clumpiness of the interstellar medium (ISM). The polarization map for Model C, in which the ISM is clumpy, is shown in Figure 3. A polarization degree of up to $\sim 4\%$ is found, which is consistent with the observational result of Fendt et al. (1996). Figure 4 shows the polarization map for Model D. The resulting degree of polarization in both models is higher than in Figure 2. It is also found that a clumpier model (Model D) always yields higher polarization than a less

clumpy model (Model C) under the same magnetic field structure. The degree of polarization appears to be equal to or greater than 4% only when both the dichroic extinction and clumpiness are taken into account. We also note that the overall extent of the galaxy map is larger than those in Figures 1 and 2. This is because the clumpier medium results in less efficient absorption and more extended scattering features compared to the smoother medium. We obtained similar polarization patterns even when the model parameters were adjusted to make the resulting surface brightness map resemble that shown in Figures 1 and 2.

4. DISCUSSION

In this study, we developed radiative transfer models which reproduce the overall structure of the optical polarization maps observed in NGC 891. We found that the extended optical polarization provides strong evidence for the existence of the extraplanar dust which has been inferred from the observations of ultraviolet reflection halos.

There is further evidence suggesting the existence of a thick dust disk. Hodges-Kluck & Bregman (2014) examined the possibility that the UV halos in highly-inclined galaxies originate from stars in the halos. However, they found that the dust scattering nebula model is most consistent with the UV observations. Observations in the mid-IR and far-IR (FIR) wavelengths also provide evidence of the extraplanar dust (Alton et al. 2000; Irwin & Madden 2006; Burgdorf et al. 2007; Verstappen et al. 2013; Bocchio et al. 2016). In particular, Bocchio et al. (2016) found that the FIR emission in NGC 891 is best fit with the sum of a thin and a thick dust component, and the scale height of the thick dust component was consistent with the result given by Seon et al. (2014).

Seon et al. (2014) found that the UV halos in NGC 891 were well reproduced by a radiative transfer model with two exponential dust disks, one with a scale height of $\approx 0.2\text{--}0.25$ kpc and the other with a scale height of $\approx 1.2\text{--}2.0$ kpc. The central face-on optical depth of the geometrically thick disk was found to be $\approx 0.3\text{--}0.5$ at the B band ($\approx 0.23\text{--}0.38$ at V). In this study, we demonstrated that the extended polarization structures can be well reproduced by thick dust disk with a scale height of 1.6 kpc and a central face-on optical depth of 1.3 at V. We also varied the scale height and optical depth of the thick dust disk within the ranges found in Seon et al. (2014). The degree of polarization was slightly lowered as the optical depth or the scale height was altered. However, no significant difference was found.

The observed polarization vectors, especially at V-band, are in general parallel to the galactic plane in the central part, but perpendicular to the galactic plane in the outer regions. Therefore, we may conclude that the magnetic fields are in general vertical (or poloidal) except the central part, where the magnetic fields are mainly toroidal. This is consistent with the result obtained from polarized radio emission (Sukumar & Allen 1991; Dumke et al. 1995; Krause 2009). It is clear that the vertical polarizations in the outer regions can mostly be attributed to scattered starlight. However, without the effect of dichroic extinction and/or clumpiness, the predicted degree of polarization is slightly lower than the observed values (middle panel of Figure 2). In our models, both the dichroic polarization and the clumpiness are also required to reproduce the observed polarization of up to 4% (Fendt et al. 1996).

However, it is noteworthy that Montgomery & Clemens

(2014) found a different V- and H-band orientation pattern in the outer disk of NGC 891. They argue that polarization vectors are unreliable tracers of the magnetic field. The optical polarization vector orientation on the northeast side of the galaxy appears to differ between Scarrott & Draper (1996) and Fendt et al. (1996). Therefore, a definite conclusion on the magnetic field orientation cannot be drawn from the V-band data alone. We also note that the polarization vector within the dust lane will be very low or erratic if a large-scale magnetic field is absent or the magnetic fields are more or less random in the central region. This would be the case of NGC 891, in which no clear pattern of polarization vectors are found in the dust lane (Scarrott & Draper 1996; Fendt et al. 1996).

The maximum degree of polarization for a single scattering in our dust model is only marginally lower than that calculated in White (1979), but significantly greater than the model of Weingartner & Draine (2001). For instance, the maximum polarization degree at the V band is 36% in our dust model, while 38% and 24% were found in the models of White (1979) and Weingartner & Draine (2001), respectively. The dust model of White (1979) used the same MRN's size distribution of dust grains, but adopted different dielectric constants than ours. The polarization degree due to dichroic extinction assumed in Wood & Jones (1997) is $P_V = 1.3\tau_V^{3/4}$ (%), which is lower than the relation ($P_V = 2.7\tau_V^{0.48}$) used in this study. It was found that the degree of dichroic polarization

was $P_V = 2.2\tau_V^{3/4}$ (%) if the polarization relation at K obtained in Jones (1989a) and the MRN dust model are combined in deriving the relation. The differences are mainly caused by uncertainties in the polarization relation and the dust extinction cross section. The overall polarization level was slightly reduced when the relation $P_V = 1.3\tau_V^{3/4}$ (%) was adopted, but no substantial difference was found.

Note that we assumed spherical dust grains when calculating the Mueller matrix and adopted an empirical approach to take into account the dichroic polarization effect. A more detailed treatment of the dichroic polarization can be found in Reissl et al. (2014) and Reissl et al. (2016). In their approach, the scattering phase function depends not only on the incident photon direction but also on the alignment of dust grains. We also note that the clumpy models (Models C and D) were devised to demonstrate that the clumpiness is also an important factor in studying polarizations. Spiral patterns were not included in the present radiative transfer models. It may be necessary to use more realistic density models. However, more detailed models are beyond the scope of the present work.

This work was supported by the National Research Foundation of Korea (NRF) grant funded by the Korea government (MSIP) (No. 2017R1A2B4008291). Numerical simulations were partially performed by using a high performance computing cluster at the Korea Astronomy and Space Science Institute.

REFERENCES

- Alton, P. B., Xilouris, E. M., Bianchi, S., Davies, J., & Kylafis, N. 2000, *A&A*, 356, 795
- Baes, M., Verstappen, J., De Looze, I., et al. 2011, *ApJS*, 196, 22
- Bianchi, S., Ferrara, A., & Giovanardi, C. 1996, *ApJ*, 465, 127
- Bocchio, M., Bianchi, S., Hunt, L. K., & Schneider, R. 2016, *A&A*, 586, A8
- Burgdorf, M., Ashby, M. L. N., & Williams, R. 2007, *ApJ*, 668, 918
- Draine, B. T. 2003, *ApJ*, 598, 1026
- Draine, B. T., & Lee, H. M. 1984, *ApJ*, 285, 89
- Draper, P. W., Done, C., Scarrott, S. M., & Stockdale, D. P. 1995, *MNRAS*, 277, 1430
- Dumke, M., Krause, M., Wielebinski, R., & Klein, U. 1995, *A&A*, 302, 691
- Fendt, C., Beck, R., Lesch, H., & Neininger, N. 1996, *A&A*, 308, 713
- Gordon, K. D., Misselt, K. A., Witt, A. N., & Clayton, G. C. 2001, *ApJ*, 551, 269
- Hodges-Kluck, E., & Bregman, J. N. 2014, *ApJ*, 789, 131
- Hodges-Kluck, E., Cafmeyer, J., & Bregman, J. N. 2016, *ApJ*, 833, 58
- Howk, J. C., & Savage, B. D. 1997, *AJ*, 114, 2463
- . 1999, *AJ*, 117, 2077
- . 2000, *AJ*, 119, 644
- Irwin, J. A., & Madden, S. C. 2006, *A&A*, 445, 123
- Jones, T. J. 1989a, *ApJ*, 346, 728
- . 1989b, *AJ*, 98, 2062
- . 1997, *AJ*, 114, 1393
- Krause, M. 2009, *RMxAC*, 36, 25
- Lazarian, A., & Hoang, T. 2007, *MNRAS*, 378, 910
- Mathis, J. S., Rumpl, W., & Nordsieck, K. H. 1977, *ApJ*, 217, 425
- Montgomery, J. D., & Clemens, D. P. 2014, *ApJ*, 786, 41
- Peest, C., Camps, P., Stalevski, M., Baes, M., & Siebenmorgen, R. 2017, *A&A*, 601, A92
- Reissl, S., Wolf, S., & Brauer, R. 2016, *A&A*, 593, A87
- Reissl, S., Wolf, S., & Seifried, D. 2014, *A&A*, 566, A65
- Roberge, W. G. 1996, in *Polarimetry of the interstellar medium*. Astronomical Society of the Pacific Conference Series; Vol. 97; Proceedings of a conference held at Rensselaer Polytechnic Institute; Troy; New York; 4-7 June 1995; San Francisco: Astronomical Society of the Pacific (ASP); lc1996; edited by Wayne G. Roberge and Doug C. B. Whittet, 401
- Rossa, J., Dettmar, R.-J., Walterbos, R. A. M., & Norman, C. A. 2004, *AJ*, 128, 674
- Scarrott, S. M. 1996, *QJRAS*, 37, 297
- Scarrott, S. M., & Draper, P. W. 1996, *MNRAS*, 278, 519
- Scarrott, S. M., Rolph, C. D., & Semple, D. P. 1990, in *IN: Galactic and intergalactic magnetic fields; Proceedings of the 140th Symposium of IAU, Durham, University, England, 245-251*
- Seon, K.-I. 2015, *JKAS*, 48, 57
- Seon, K.-I., & Draine, B. T. 2016, *ApJ*, 833, 201
- Seon, K.-I., & Witt, A. N. 2012, *The Spectral Energy Distribution of Galaxies*, 284, 135
- Seon, K.-I., Witt, A. N., Shinn, J.-H., & Kim, I.-J. 2014, *ApJ*, 785, L18
- Shinn, J.-H., & Seon, K.-I. 2015, *ApJ*, 815, 133
- Steinacker, J., Baes, M., & Gordon, K. D. 2013, *ARA&A*, 51, 63
- Sukumar, S., & Allen, R. J. 1991, *ApJ*, 382, 100
- Thompson, T. W. J., Howk, J. C., & Savage, B. D. 2004, *AJ*, 128, 662
- Verstappen, J., Fritz, J., Baes, M., et al. 2013, *A&A*, 556, 54
- Weingartner, J. C., & Draine, B. T. 2001, *ApJ*, 548, 296
- White, R. L. 1979, *ApJ*, 229, 954
- Whittet, D. C. B., Hough, J. H., Lazarian, A., & Hoang, T. 2008, *ApJ*, 674, 304
- Wood, K. 1997, *ApJL*, 477, L25
- Wood, K., & Jones, T. J. 1997, *AJ*, 114, 1405
- Xilouris, E. M., Byun, Y. I., Kylafis, N. D., Paleologou, E. V., & Papamastorakis, J. 1999, *A&A*, 344, 868

TABLE 1
MODEL PARAMETERS

Parameter		Model A	Model B, C, D
Scale height of stellar disk	Z_s	0.4	0.4
Scale length of stellar disk	R_s	5.4	5.4
Bulge to total luminosity ratio	B/T	0.3	0.2
Bulge effective radius	R_e	1.5	1.0
Bulge axial ratio	q	0.5	0.5
Optical depth of thin dust disk	τ_V^{thin}	0.8	0.8
Scale height of thin dust disk	Z_d^{thin}	0.25	0.25
Scale length of thin dust disk	R_d^{thin}	7.7	7.7
Optical depth of thick dust disk	τ_V^{thick}		0.3
Scale height of thick dust disk	Z_d^{thick}		1.6
Scale length of thick dust disk	R_d^{thick}		7.7
Inclination angle	θ_{inc}	89.8	89.8

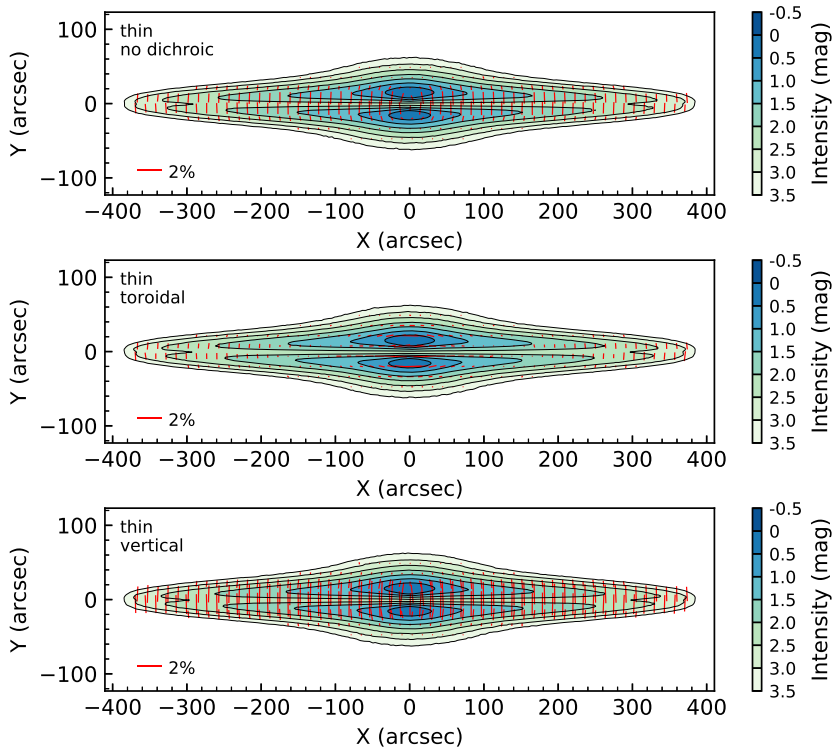


FIG. 1.— V-band polarization maps for Model A in which only a thin dust disk is considered. (top) No dichroic extinction is included. (middle) Magnetic field is assumed to be toroidal (parallel to the galactic plane). (bottom) Magnetic field is assumed to be vertical (perpendicular to the plane). The intervals between contours are in units of half-magnitude.

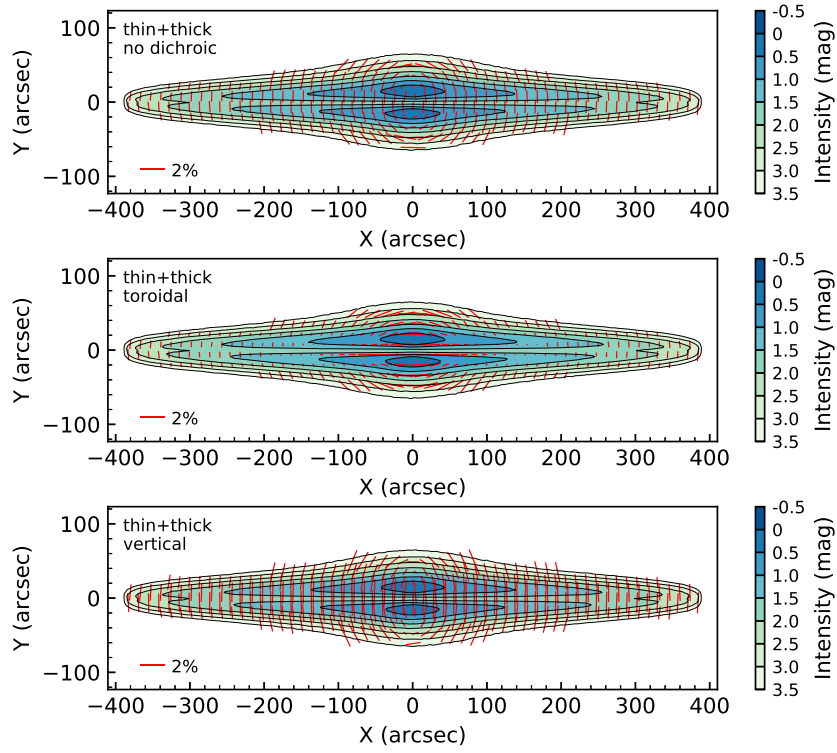


FIG. 2.— V-band polarization maps for Model B in which both thin and thick dust disks are considered. (top) No dichroic extinction is included. (middle) Magnetic field is assumed to be toroidal (parallel to the galactic plane). (bottom) Magnetic field is assumed to be vertical (perpendicular to the plane).

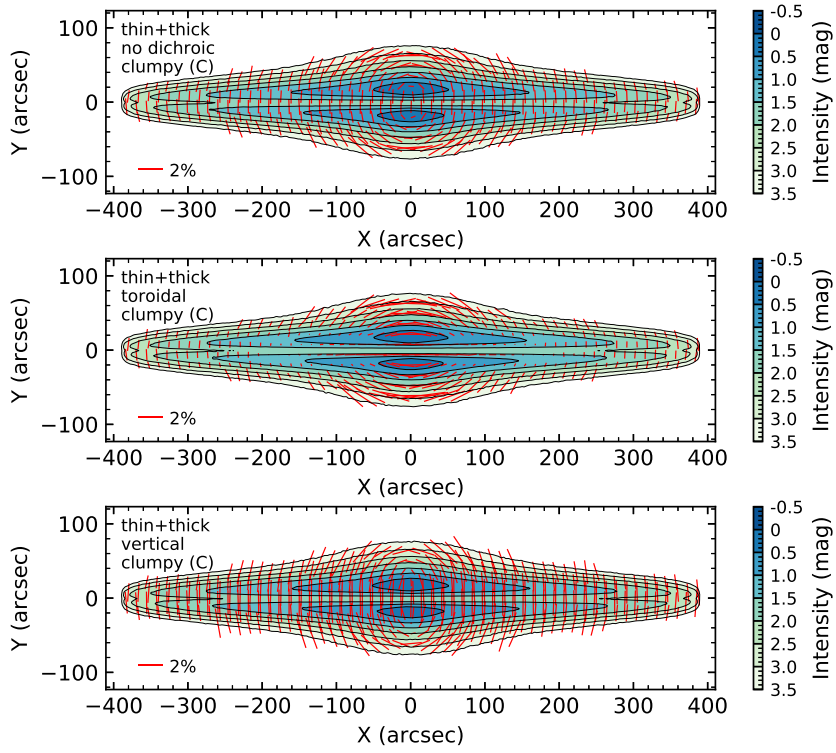


FIG. 3.— V-band polarization maps for Model C in which the medium is assumed to be clumpy. Magnetic field is assumed to be vertical. (top) No dichroic extinction is included. (middle) Magnetic field is assumed to be toroidal (parallel to the galactic plane). (bottom) Magnetic field is assumed to be vertical (perpendicular to the plane).

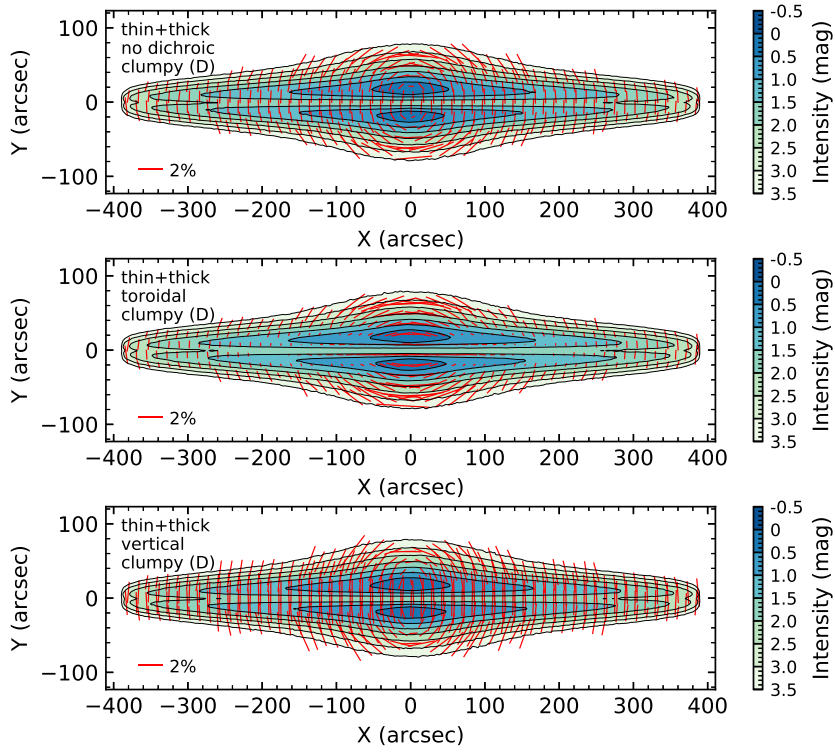


FIG. 4.— V-band polarization maps for Model D in which the medium is assumed to be clumpy. Magnetic field is assumed to be vertical. The medium for Model D is clumpier than that for Model C. (top) No dichroic extinction is included. (middle) Magnetic field is assumed to be toroidal (parallel to the galactic plane). (bottom) Magnetic field is assumed to be vertical (perpendicular to the plane).